Published in final edited form as:
J Biomech. 2008 November 14; 41(15): 3158–3163. doi:10.1016/j.jbiomech.2008.08.020.

Micromechanical modeling of the cement-bone interface: the effect of friction, morphology and material properties on the micromechanical response

Dennis Janssen[1,2], **Kenneth A. Mann**[2], and **Nico Verdonschot**[1,3]

[1] *Radboud University Nijmegen Medical Centre, Orthopaedic Research Laboratory, Nijmegen, The Netherlands* [2] *SUNY Upstate Medical University, Syracuse, NY, USA* [3] *University of Twente, Laboratory for Biomechanical Engineering, Enschede, The Netherlands*

Abstract

In order to gain insight into the micro-mechanical behavior of the cement-bone interface, the effect of parametric variations of frictional, morphological and material properties on the mechanical response of the cement-bone interface were analyzed using a finite element approach. Finite element models of a cement-bone interface specimen were created from micro-computed tomography data of a physical specimen that was sectioned from an in vitro cemented total hip arthroplasty. In five models the friction coefficient was varied (μ= 0.0; 0.3; 0.7; 1.0 and 3.0), while in one model an ideally bonded interface was assumed. In two models cement interface gaps and an optimal cement penetration were simulated. Finally, the effect of bone cement stiffness variations was simulated (2.0 and 2.5 GPa, relative to the default 3.0 GPa). All models were loaded for a cycle of fully reversible tension-compression. From the simulated stress-displacement curves the interface deformation, stiffness and hysteresis were calculated. The results indicate that in the current model the mechanical properties of the cement-bone interface were caused by frictional phenomena at the shape-closed interlock rather than by adhesive properties of the cement. Our findings furthermore show that in our model maximizing cement penetration improved the micromechanical response of the cement-bone interface stiffness, while interface gaps had a detrimental effect. Relative to the frictional and morphological variations, variations in the cement stiffness had only a modest effect on the micromechanical behavior of the cement-bone interface. The current study provides information that may help to better understand the load transfer mechanisms taking place at the cement-bone interface.

Keywords

bone; bone cement; finite element; interface

Introduction

In cemented total hip arthroplasty, fixation of the implants in the bone is achieved by bone cement inserted in a doughy form at the time of operation. The cement subsequently penetrates

Correspondence: Dennis Janssen, Radboud University Nijmegen Medical Centre, Orthopaedic Research Laboratory, P.O. Box 9101, 6500 HB Nijmegen, The Netherlands, Tel. +31 24 36 16959, Fax. +31 24 35 40555, Email d.janssen@orthop.umcn.nl.

into bone lacunar and trabecular spaces, forming a complex interlock between the cement and bone, ensuring fixation of the cement mantle within the bone.

Much research has been conducted to determine the strength of the cement-bone interface (Arola et al., 2006; Bean et al., 1987; Dohmae et al., 1988; Funk and Litsky, 1998; Kim et al., 2004; Krause et al., 1982; Mann et al., 1997). However, these studies simplify the cement-bone interface to an apparent level, whereas in reality this interface is a morphologically complex cement-bone composite.

Recently, experiments have been performed to determine the micromechanical behavior of the cement-bone interface (Mann et al., 2008). Interface specimens were subjected to nondestructive fully reversible tension-compression loads, while the local micromotions of the cement, bone and cement-bone interface were monitored. The results showed that the interface is more compliant than the cement and bone. Substantial hysteresis occurred during one tension-compression cycle, attributed to sliding contact at the interface. It remains, however, unclear how loads are transferred across the interface, as this could not be assessed.

Cement-bone adhesion may play a role in the mechanical response observed experimentally, although it may be compromised by fat, blood and other fluids that are present in the bone during cement insertion. On the other hand, the micromechanical behavior of the cement-bone interface may also be attributed to the shape-closed interlock of cement penetrated into the bone trabecular and lacunar spaces, combined with frictional phenomena.

In addition to this, variations in the cement-bone interface morphology may affect the micromechanical response of the shape-closed interlock. For instance, more cement penetration may enhance the mechanical properties of the interface. On the other hand, cement is known to shrink during polymerization (Davies and Harris, 1995; Hamilton et al., 1988), which may cause gaps to occur at the cement-bone interface, causing inferior mechanical properties at the interface.

A third possible factor affecting the micromechanical behavior of the cement-bone interface is the variability of cement material properties. Lower modulus cement has been considered as an approach to reduce interface stresses (Funk and Litsky, 1998). The stiffness of commercially available bone cements varies between roughly 2.0 and 3.0 GPa (Lewis, 1997). The effect of this variation on the actual micromechanical response of the cement-bone interface is unclear.

In order to gain insight in the micro-mechanical behavior of the cement-bone interface we developed a micromechanical finite element analysis (FEA) model based on an experimental cement-bone interface specimen (Mann et al., 2008) and analyzed the effect of parametric variations of frictional, morphological and material properties on the mechanical response. We asked the following questions: (1) Are the mechanical properties of the cement-bone interface caused by frictional phenomena via shape-closed mechanical interlock or by adhesive properties of the cement?; (2) How do interface morphological variations affect the micromechanical response of the cement-bone interface?; (3) How do variations in cement stiffness affect the micromechanical response of the cement-bone interface?

Methods

The FEA models used for the parametric analyses were created from micro computed tomography (μCT) scans of a cement-bone interface specimen (Figure 1a) that was previously tested experimentally (Mann et al., 2008). The specimen (5×5×10 mm) was sectioned from a cemented total hip arthroplasty in a fresh-frozen proximal human cadaver femur. The specimen

was μCT-scanned at a 12 μm isotropic resolution (Scanco μCT 40, Scanco Medical AG, Basserdorf, Switzerland; Figure 1b).

FEA meshes were created using commercial software (Mimics 11.1, Materialise, Leuven, Belgium). The cement and bone were segmented based upon the image grayscale. In general, the segmented cement and bone consisted of one large part and some small parts. The smaller parts were removed by performing a region growing operation. Next, a one-voxel erosion operation was performed on the cement to prevent interpenetration between cement and bone. Surface models were generated for cement and bone. To keep element number to a tractable level the triangular surface meshes were generated after a 6×6×6 voxel reduction. The surface meshes were remeshed to reduce the number of elements and generate element shapes with appropriate aspect ratios. Four-node tetrahedral meshes were created from the surface meshes (Patran 2005r2, MSC Software Corporation, Santa Ana, CA, USA). The resulting model existed of approximately 335,000 elements and 80,000 nodes (Figure 1c), and was regarded as the “normal” interface morphology model.

The bone and cement were considered to be linear elastic. The bone properties were assigned based upon μCT grayscale values, which were converted to equivalent HA-densities using a calibration phantom. A linear relationship between the HA-density and the Young’s modulus was assumed (Lotz et al., 1991), resulting in stiffness values ranging from 0.1 to 20.0 GPa (ν=0.3). The cement was assumed to have uniform material properties (E=3.0 GPa; ν=0.3; Simplex P, Stryker Orthopaedics, Mahwah, NJ, USA).

Contact between the cement and bone was modeled using a double-sided node-to-surface contact algorithm (MSC.MARC 2005r3, MSC Software Corporation, Santa Ana, CA, USA). The contact algorithm simulated contact between nodes of one contact body and the element surface of the other body. The detection and implementation of contact and friction was achieved through a direct constraint model. In order to study the effect of cement adhesion in one model an ideally bonded contact interface was simulated. Adhesion was only simulated in areas where no gaps were present. In these areas, direct constraints placed on the nodes were adapted such that no relative tangential and normal motions could occur. To study the effect of friction, we varied the friction coefficient in five other models (μ = 0.0; 0.3; 0.7; 1.0 and 3.0). Friction was modeled using a bilinear Coulomb friction model. This model is based on relative tangential displacements, and assumes that stick and slip conditions correspond to reversible (elastic) and permanent (plastic) relative displacements.

In two models the effect of morphological variations was studied. In the first model the effect of additional gaps at the contact interface was simulated, representing an interface achieved by an inferior cementing technique. Due to absence of morphological data we chose a numerical approach to simulate interface gaps. We applied an additional one-voxel erosion operation, causing an additional gap of roughly 12 μm at the cement bone interface. In a second model, optimal cement penetration was simulated by filling all bone lacunar cavities with cement, even at locations where no cement was present according to the μCT data.

Finally, two models were analyzed in which low and intermediate stiffness bone cement was simulated (Young’s modulus of 2.0 and 2.5 GPa, respectively). In models with morphological and cement stiffness variations frictional contact was assumed with the default friction coefficient (0.3).

All models were loaded for one cycle of fully reversible tension-compression, mimicking the experimental protocol (Mann et al., 2008). During the simulation, the distal end of the cement was fixed in all directions, while the proximal end of the bone was displaced in the longitudinal direction (Figure 1c). The proximal end was fixed such that tilting was restricted, while displacement in the transversal directions was allowed. Incremental displacement steps of 1.0

μm were applied until the maximal experimental levels of tension (1.04 MPa) and compression (−2.03 MPa) were reached (Figure 2).

In the experiments, digital image correlation techniques were used to quantify bone, interface and cement deformations (Mann et al., 2008). Twelve sampling points were taken (Figure 1a): three columns of four sampling points located in the bone (two points) and the cement (two points). By tracking the relative displacements of the bone points the local deformation of the bone was calculated. In the same manner the deformation of the cement and interface were calculated. This was done for the three columns, after which the calculated deformations of the cement, bone and contact interface were averaged to establish the 'global' deformations. To enable direct comparison of the mechanical behavior of the models relative to the experiments, the same locations were used in the models to calculate deformation.

We determined stress-displacement curves and calculated the interface stiffness in tension and compression by fitting linear lines through the curves. Consistent with the experimental study (Mann et al., 2008) the stiffness was expressed as the ratio of the applied stress and the deformation (MPa/mm) instead of the strain at the interface, since discontinuities in the interface materials and morphology prevented the use of an unambiguous strain measure. Finally, we calculated the horizontal span of the stress-displacement curves, which served as a measure for hysteresis occurring in the models (Figure 2).

Results

In cases where the cement-bone interface was assumed to be unbonded, the cement-bone interface deformed in a non-homogeneous manner. For example, during application of the tensile load, the cement and bone remained in contact at some locations, while at other locations gaps occurred (Figure 3). The normal morphology model with a friction coefficient of 0.3 resulted in a micromechanical response at the cement-bone interface that was similar to the experiment (Figure 4). In all models, the majority of the deformation took place at the contact interface, both in tension (90%) and compression (87%); this was consistent with the experimental results. In addition, the cement-bone interface was found to be more compliant in tension than in compression.

The mechanical response of the parametric studies is presented in terms of interface deformation (Table 1), interface stiffness in tension and compression (Figure 5), and horizontal span (Figure 6).

Increasing the friction coefficient generally decreased the deformation at the interface and increased the interfacial stiffness, both in compression and tension. The horizontal span decreased with increasing friction coefficient. An ideally bonded contact interface decreased the interface deformation and the horizontal span, and furthermore resulted in a response that was much stiffer than the unbonded cases. The results of the unbonded models with relatively low friction coefficient values (0.0 to 0.7) more closely approximated the experimental values than those of models with a relatively high friction coefficient (1.0 and 3.0), or with a bonded interface.

Changes in morphology at the contact interface had a dramatic effect on the interface deformation. Introduction of interface gaps increased interface motion, decreased stiffness and increased the horizontal span when compared to the normal morphology case. Filling gaps with cement had the opposite effect.

Compared to the frictional and morphological variations, reducing the cement stiffness had only a modest, but somewhat predictable effect on the mechanical response. Application of low modulus cement (with a cement stiffness decrease of 33%) decreased the tensile interface

stiffness by 27% relative to the high stiffness cement. Decreasing the cement stiffness led to an increased interface deformation, reduced interface stiffness and increased horizontal span.

Discussion

In the current study, we analyzed the effect of parametric variations of frictional, morphological and material properties on the mechanical response of a cement-bone interface.

Our results show that when an ideally bonded contact interface was assumed, the deformation at the interface was underestimated with respect to the experimental values. Furthermore, interface stiffness was overestimated in tension and compression, and hysteresis was underestimated. These results suggest the micromechanical behavior of the cement-bone interface is caused by frictional phenomena rather than by adhesive properties of the cement. Previously, authors have reported on the limited adhesive properties of cement relative to bone (Lucksanasombool et al., 2003; Skipritz and Aspenberg, 1999). Considering the presence of fluids in the bone (blood, fat, marrow) at the time of cement insertion, the assumption that cement does not adhere to the bone seems very plausible.

Morphological variations had a substantial effect on the micromechanical response of the cement-bone interface. Simulating additional interface gaps reduced the interface stiffness and resulted in large interface deformations. The interface gap led to a span of approximately 12 μm, which can be attributed to the additional erosion process. In contrast, a maximal cement fill increased the cement-bone interface stiffness and decreased the deformation. Previously, it has been shown that maximizing bone-cement interdigitation increases the strength of the interface (Bean et al., 1987; Krause et al., 1982; Mann et al., 1997). These findings stress the importance of cement pressurization during the preparation of a cemented total hip reconstruction.

Compared to the frictional and morphological properties of the interface, the effect of cement stiffness was rather small. In our models, increasing the cement stiffness increased the stiffness and reduced hysteresis. The stiffness reduction was proportional to the cement stiffness reduction. Funk et al. (1998) showed a 50% interface shear stiffness reduction with low-stiffness PBMMA (polybutyl methyl methacrylate) cement compared to normal PMMA (polymethyl methacrylate) cement. However, the Young's modulus of the low-stiffness PBMMA cement was almost 8 times lower than that of normal cement. The discrepancy between that study and current findings may be attributed to differences in the loading, material properties or method of preparation of the experimental specimens.

Our study was limited by the fact that a single cement-bone interface specimen was used for the parametric variations. The specimen was chosen from a batch of 21 specimens used previously for experimental testing (Mann et al, 2008). That study showed the stiffness of the cement-bone interface is proportional to the level of cement interdigitation, with values ranging from 61.7 to 630.3 MPa/mm. This large range indicates the substantial effect of morphological variations on the micromechanical behavior; variations that were not included in the current study. In a separate study we modeled ten of the experimental specimens with frictional contact at the contact interface (friction coefficient of 0.3). The results of that study indicated that using frictional contact did not lead to an underprediction of the stiffness that was measured experimentally, which further confirms our assumption that the cement does not adhere to the bone.

In order to limit the number of elements, the μCT data was reduced prior to surface meshing. Subsequently, the surface models were remeshed to improve the mesh quality and to further reduce the number of elements. These operations may have introduced errors in some parts of the models. Consequentially, smaller cement parts penetrating into the bone may have been

lost or underrepresented due to the meshing process. Despite the errors the current models were able to approximate the micromechanical behavior of the experimental cement-bone interface specimen. This suggests that the micromechanical behavior depends mainly on the interlock of the larger structures present at the interface. Increasing the μCT resolution and the number of elements in the models should, however, result in a more accurate prediction of the interface micromechanics.

In order to prevent interpenetration between the cement and bone we applied a one-voxel erosion operation on the cement. Initial models in which this operation was not applied showed that interpenetration caused artificial stiffening of the contact interface. It was not possible to resolve this by adjusting the contact procedure (for instance by simulating initial stress-free contact). Projection of the mesh on the initial μCT-data indicated that the application of the erosion process led to a more accurate morphological description of the specimen. Furthermore, our results indicated that the eroded model gave a better prediction of the micromechanical behavior as shown experimentally. The effect of the erosion process is reflected best by the comparison between the span produced by our "normal" and "gaps" models. While the standard 12 μm erosion process led to only a relatively small span (approx. 3 μm), the additional erosion process applied to the "gaps" model produced much more play (approx. 12 μm). This illustrates that, as intended, our standard one-pixel erosion process removed the mesh interpenetration without introducing excessive play at the interface, whereas introducing an additional gap resulted in a substantial increase of the span.

When assigning bone material properties based upon CT-grayscale, it is common to use a power law relating the bone density to a certain Young's modulus (Carter and Hayes, 1977; Keller et al., 1994; Wirtz et al., 2000). In case of models based upon μCT data sometimes a constant tissue modulus is used (Hou et al., 1998; van Rietbergen et al., 1995). In the current study, a linear relationship between the bone density and the Young's modulus was assumed (Lotz et al., 1991). Preliminary analyses with models using a number of different modulus-density relationships for bone showed that the material law had only a minor effect on the mechanical behavior of the cement-bone interface.

Since linear elastic isotropic material properties were used for the cement and bone, the FEA models were unable to simulate viscoelastic material behavior that may have occurred in the experiments. This difference may explain why hysteresis (horizontal span in the stress-displacement curves) was generally underestimated by the current models. In addition, no damage was simulated at the cement-bone contact interface, although in some small parts rather high Von Mises stress levels (> 150 MPa) were found, both in the cement and bone. This may provide an additional explanation for the discrepancy between the numerical and experimental findings.

To our knowledge, this is the first publication reporting a simulation of the micromechanical behavior of the cement-bone interface. Previously, authors have modeled debonding processes of the stem-cement interface (Perez et al., 2006a, 2006b; Verdonschot and Huiskes, 1997a, 1997b). Furthermore, research has been conducted on the micromotions and osseointegration of the implant-bone interface in case of uncemented implants (Moreo et al., 2007; Rubin et al., 1993; Spears et al., 2001). The current study provides information that may help to better understand the load transfer mechanisms taking place at the cement-bone interface.

In conclusion, the results of this study indicate that in the current model, (1) the mechanical properties of the cement-bone interface were caused by frictional phenomena at the shape-closed mechanical interlock rather than by adhesive properties of the cement. (2) Our findings furthermore showed that in the current model maximizing cement penetration and local apposition increased the cement-bone interface stiffness, while interface gaps had a detrimental

effect on its micromechanical behavior. (3) Relative to the frictional and morphological variations, variations in the cement stiffness had only a modest effect on the micromechanical behavior of the cement-bone interface.

Acknowledgements

This work was funded by NIH-NIAMS AR42017.

References

Arola D, Stoffel KA, Yang DT. Fatigue of the cement/bone interface: the surface texture of bone and loosening. Journal of Biomedical Materials Research Part B: Applied Biomaterials 2006;76:287–297.

Bean DJ, Convery FR, Woo SL, Lieber RL. Regional variation in shear strength of the bone-polymethylmethacrylate interface. Journal of Arthroplasty 1987;2:293–298. [PubMed: 3430156]

Carter DR, Hayes WC. The compressive behavior of bone as a two-phase porous structure. Journal of Bone and Joint Surgery, American Volume 1977;59:954–962.

Davies JP, Harris WH. Comparison of diametral shrinkage of centrifuged and uncentrifuged Simplex P bone cement. Journal of Applied Biomaterials 1995;6:209–211. [PubMed: 7492813]

Dohmae Y, Bechtold JE, Sherman RE, Puno RM, Gustilo RB. Reduction in cement-bone interface shear strength between primary and revision arthroplasty. Clinical Orthopaedics and Related Research 1988:214–220. [PubMed: 3180573]

Funk MJ, Litsky AS. Effect of cement modulus on the shear properties of the bone-cement interface. Biomaterials 1998;19:1561–1567. [PubMed: 9830981]

Hamilton HW, Cooper DF, Fels M. Shrinkage of centrifuged cement. Orthopaedic Review 1988;17:48–54. [PubMed: 3174195]

Hou FJ, Lang SM, Hoshaw SJ, Reimann DA, Fyhrie DP. Human vertebral body apparent and hard tissue stiffness. Journal of Biomechanics 1998;31:1009–1015. [PubMed: 9880057]

Keller TS. Predicting the compressive mechanical behavior of bone. Journal of Biomechanics 1994;27:1159–1168. [PubMed: 7929465]

Kim DG, Miller MA, Mann KA. Creep dominates tensile fatigue damage of the cement-bone interface. Journal of Orthopaedic Research 2004;22:633–640. [PubMed: 15099645]

Krause WR, Krug W, Miller J. Strength of the cement-bone interface. Clinical Orthopaedics and Related Research 1982:290–299. [PubMed: 7067264]

Lewis G. Properties of acrylic bone cement: state of the art review. Journal of Biomedical Materials Research 1997;38:155–182. [PubMed: 9178743]

Lotz JC, Gerhart TN, Hayes WC. Mechanical properties of metaphyseal bone in the proximal femur. Journal of Biomechanics 1991;24:317–329. [PubMed: 2050708]

Lucksanasombool P, Higgs WA, Ignat M, Higgs RJ, Swain MV. Comparison of failure characteristics of a range of cancellous bone-bone cement composites. Journal of Biomedical Materials Research Part A 2003;64:93–104. [PubMed: 12483701]

Mann KA, Ayers DC, Werner FW, Nicoletta RJ, Fortino MD. Tensile strength of the cement-bone interface depends on the amount of bone interdigitated with PMMA cement. Journal of Biomechanics 1997;30:339–346. [PubMed: 9075001]

Mann KA, Miller MA, Cleary RJ, Janssen D, Verdonschot N. Experimental micromechanics of the cement-bone interface. Journal of Orthopaedic Research 2008;26:872–879. [PubMed: 18253965]

Moreo P, Perez MA, Garcia-Aznar JM, Doblare M. Modelling the mechanical behaviour of living bony interfaces. Computer Methods in Applied Mechanics and Engineering 2007;196:3300–3314.

Perez MA, Garcia-Aznar JM, Doblare M, Seral B, Seral F. A comparative FEA of the debonding process in different concepts of cemented hip implants. Medical Engineering & Physics 2006a:525–533.

Perez MA, Grasa J, Garcia-Aznar JM, Bea JA, Doblare M. Probabilistic analysis of the influence of the bonding degree of the stem-cement interface in the performance of cemented hip prostheses. Journal of Biomechanics 2006b;39:1859–1872. [PubMed: 16054633]

Rubin PJ, Rakotomanana RL, Leyvraz PF, Zysset PK, Curnier A, Heegaard JH. Frictional interface micromotions and anisotropic stress distribution in a femoral total hip component. Journal of Biomechanics 1993;26:725–739. [PubMed: 8514816]

Skipritz R, Aspenberg P. Attachment of PMMA cement to bone: force measurements in rats. Biomaterials 1999;20:351–356. [PubMed: 10048407]

Spears IR, Pfleiderer M, Schneider E, Hille E, Morlock MM. The effect of interfacial parameters on cup-bone relative micromotions. A finite element investigation. Journal of Biomechanics 2001;34:113–120. [PubMed: 11425070]

Van Rietbergen B, Weinans H, Huiskes R, Odgaard A. A new method to determine trabecular bone elastic properties and loading using micromechanical finite-element models. Journal of Biomechanics 1995;28:69–81. [PubMed: 7852443]

Verdonschot N, Huiskes R. Cement debonding process of total hip arthroplasty stems. Clinical Orthopaedics and Related Research 1997a;336:297–307. [PubMed: 9060516]

Verdonschot N, Huiskes R. The effects of cement-stem debonding in THA on the long-term failure probability of cement. Journal of Biomechanics 1997b;30:795–802. [PubMed: 9239564]

Wirtz DC, Schiffers N, Pandorf T, Radermacher K, Weichert D, Forst R. Critical evaluation of known bone material properties to realize anisotropic FE-simulation of the proximal femur. Journal of Biomechanics 2000;33:1325–1330. [PubMed: 10899344]

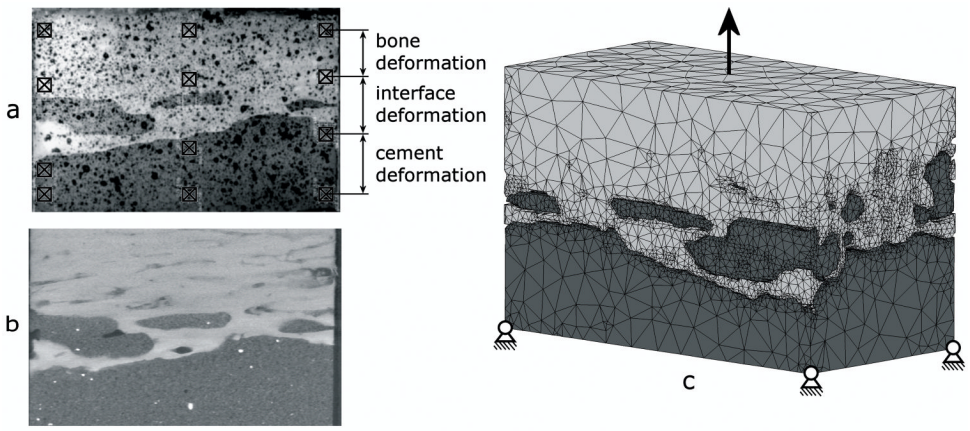

Figure 1.
(a) Image of a specimen that was tested experimentally in which the twelve DIC sampling points are indicated; (b) a μCT image of the same specimen and (c) the FEA model of the cement-bone interface specimen created from the μCT-data, with the boundary conditions indicated.

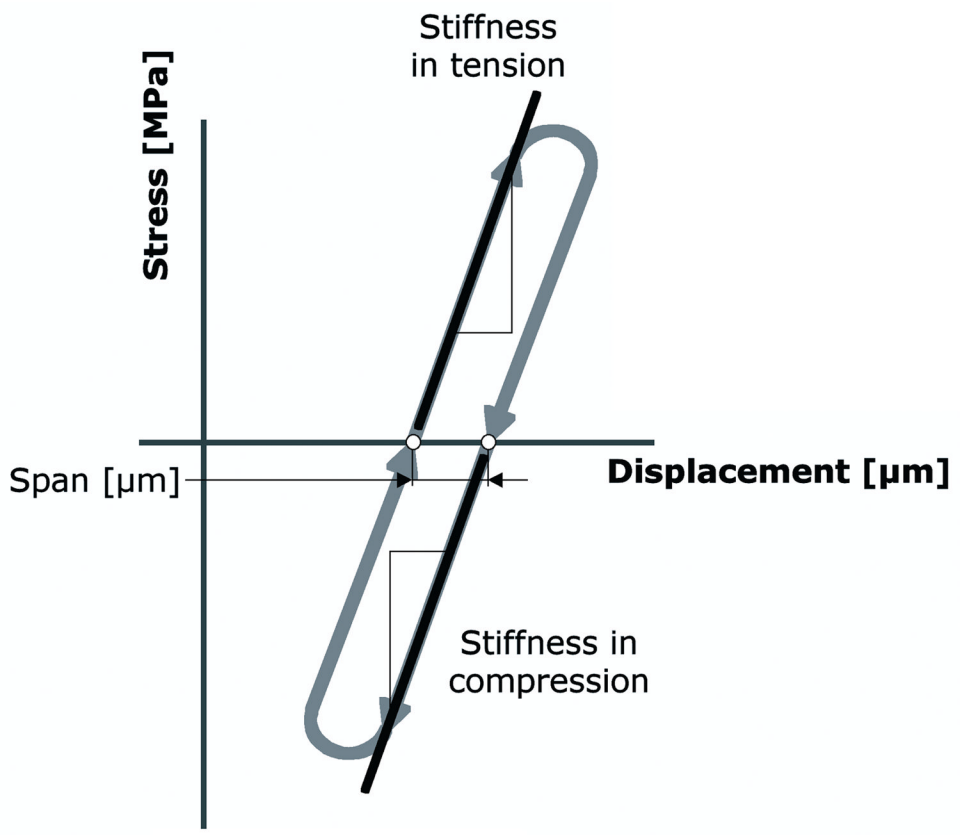

Figure 2.
Schematic stress-displacement diagram with the outcome measures used in the current study.

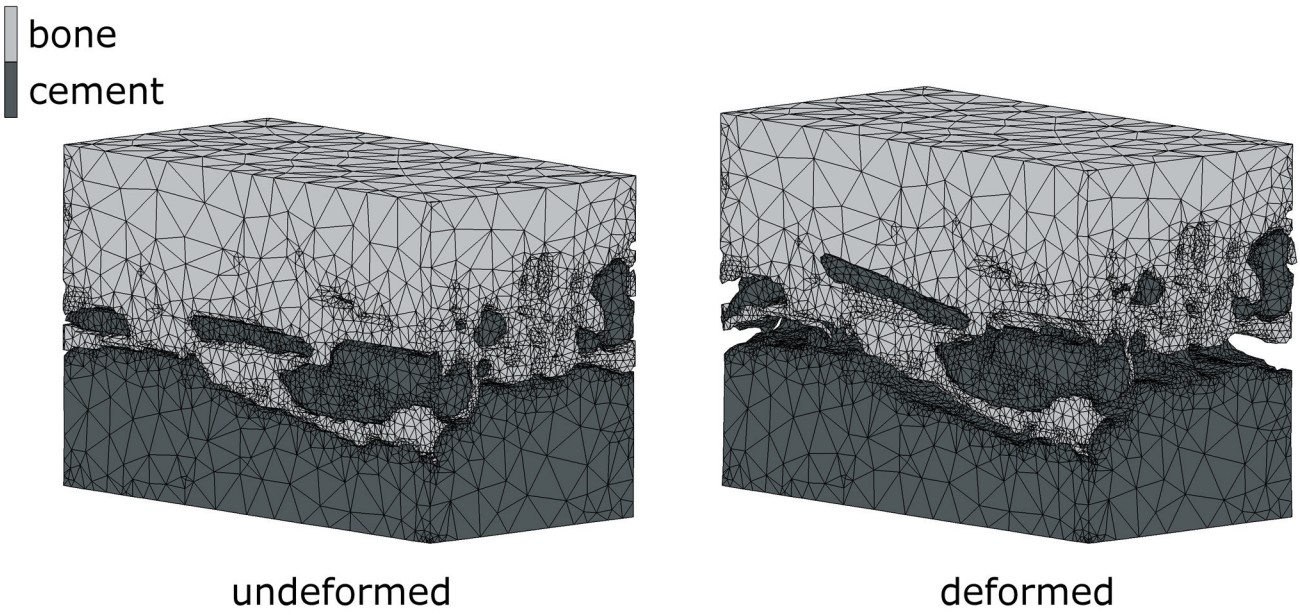

Figure 3.
FEA model in the unloaded (left) situation, and under full tension load (right). Notice that in the deformed state, gaps occurred between the cement and bone at some locations, while at other locations the cement remained in contact with the bone. In this particular case, a friction coefficient of 0.3 was modeled. The deformations are 50 times magnified for illustrative purposes.

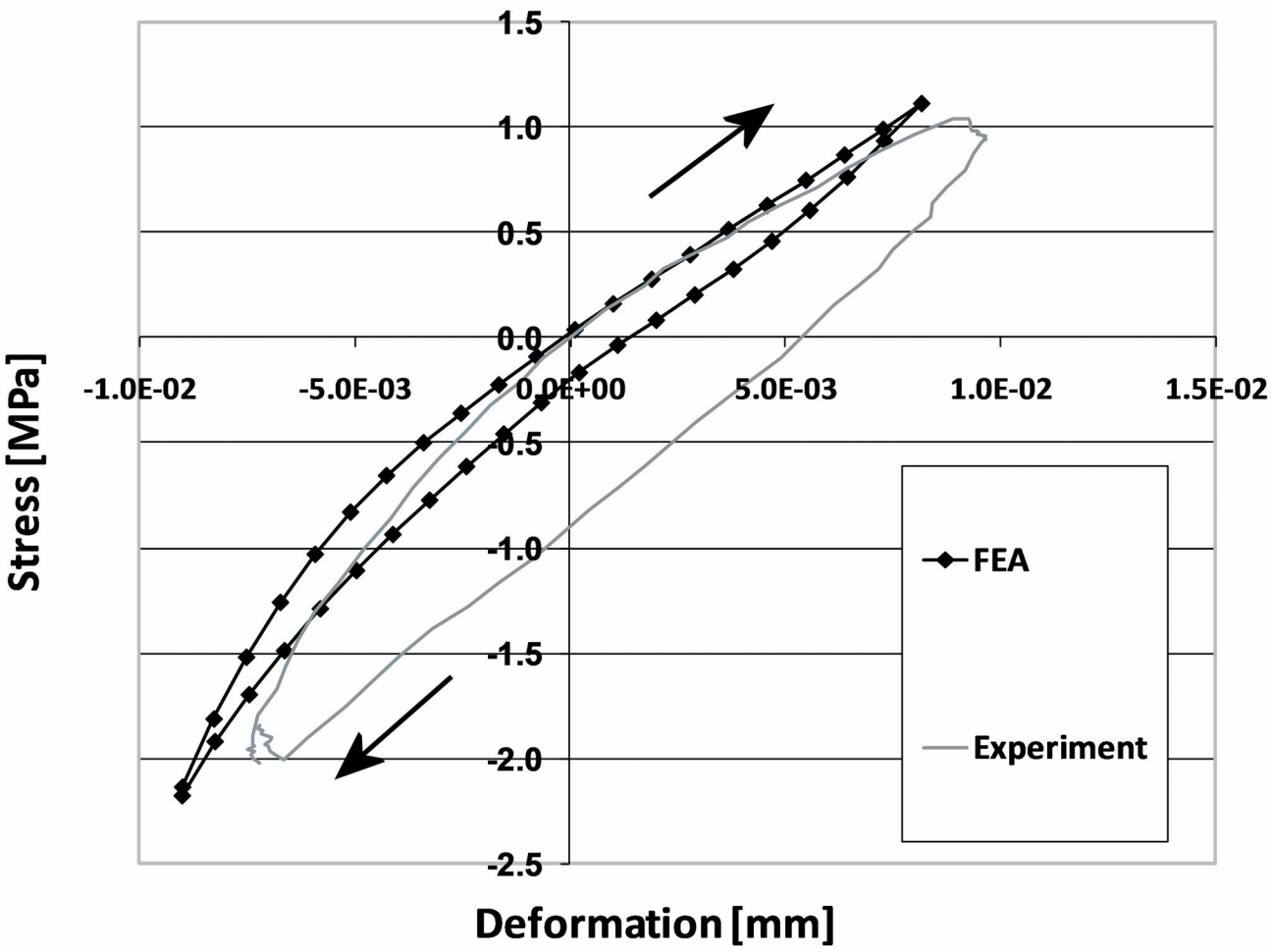

Figure 4.
Micromechanical response of the cement-bone interface from experimental results and as simulated with an FEA model with a friction coefficient of 0.3 and a normal interface morphology. The loading direction is indicated by the arrows. For illustrative purposes, both curves were shifted to make them pass through zero stress and displacement. Initial offsets due to experimental and numerical settling were omitted.

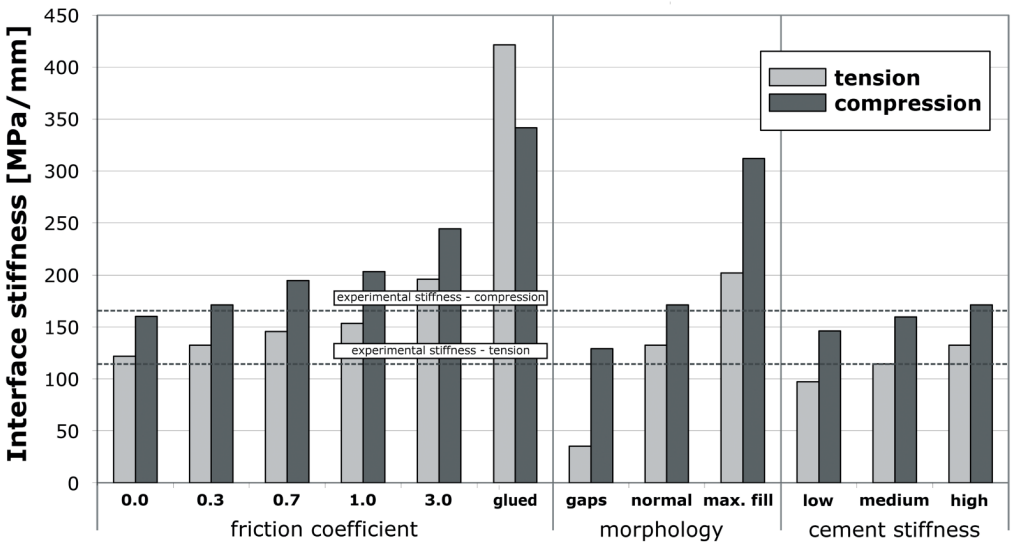

Figure 5.
Stiffness response of the cement-bone interface in tension and compression for the parametric studies.

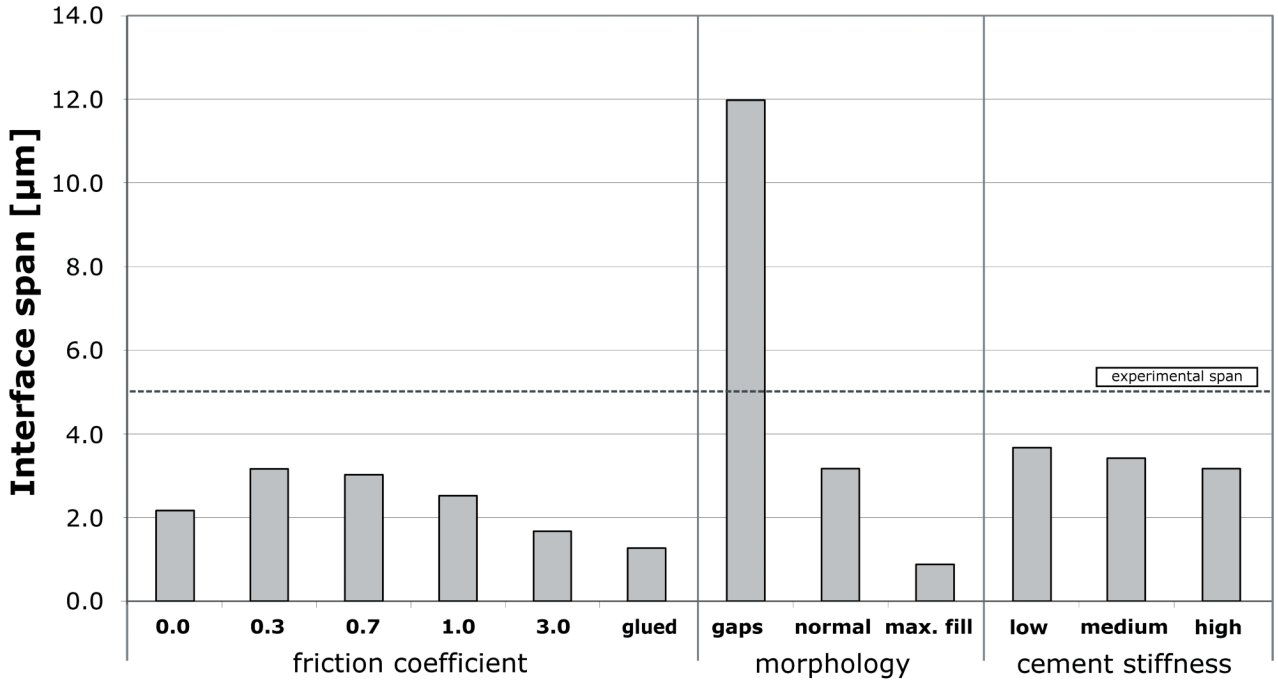

Figure 6.
Horizontal span at the cement-bone interface from the various models

Table 1

Deformation of the cement-bone interface in full tension (1.04 MPa) and compression (−2.03 MPa) for the various parametric studies.

	Interface deformation [μm]	
	Tension	**Compression**
μ = 0.0	8.10	11.95
μ = 0.3	8.05	12.03
μ = 0.7	7.10	10.98
μ = 1.0	7.05	10.11
μ = 3.0	5.13	9.04
Ideally bonded interface	2.22	6.15
Interface gaps	31.90	17.01
Normal morphology	8.05	12.03
Maximal fill	4.98	6.98
Low cement stiffness	10.73	14.34
Medium cement stiffness	8.95	12.77
High cement stiffness	8.05	12.03
Experimental results	*8.08*	*11.51*